Distribution Agreement

In presenting this thesis as a partial fulfillment of the requirements for a degree from Emory University, I hereby grant to Emory University and its agents the non-exclusive license to archive, make accessible, and display my thesis in whole or in part in all forms of media, now or hereafter now, including display on the World Wide Web. I understand that I may select some access restrictions as part of the online submission of this thesis. I retain all ownership rights to the copyright of the thesis. I also retain the right to use in future works (such as articles or books) all or part of this thesis.

Richard Nwakamma April 12, 2022

An Investigation of the domain-domain interactions of A Disintegrin Metalloproteinase domain-containing protein 10 (ADAM10)

by

Richard Nwakamma

Haian Fu
Adviser

Chemistry

Haian Fu

Adviser

David Lynn

Committee Member

Monika Raj

Committee Member

Brenda Harmon

Committee Member

2022

An Investigation of the domain-domain interactions of A Disintegrin Metalloproteinase domain-containing protein 10 (ADAM10)

By

Richard Nwakamma

Haian Fu

Adviser

An abstract of
a thesis submitted to the Faculty of Emory College of Arts and Sciences
of Emory University in partial fulfillment
of the requirements of the degree of
Bachelor of Science with Honors

Chemistry

2022

Abstract

An Investigation of the domain-domain interactions of A Disintegrin Metalloproteinase domain-containing protein 10 (ADAM10)

By Richard Nwakamma

Alzheimer's disease (AD) is the most common form of dementia and is characterized as a chronic neurodegenerative illness leading to memory loss and loss of cognitive function. A Disintegrin and Metalloproteinase domain-containing protein 10 (ADAM10) is a key protein involved in many biological processes including neuropathology, inflammatory response, and tumor progression. In neurons, ADAM10 acts as an α-secretase to mediate proteolytic processing of the amyloid precursor protein (APP). It plays a critical role in reducing the generation of amyloid-β (Aβ) peptides which helps reduce the pathogenesis of AD. ADAM10 is a membrane protein, and its extracellular component consists of four functional domains, including a pro domain (P), metalloprotease domain (M), a disintegrin domain (D) and a cysteine rich domain (C). The crystal structure of a truncated ADAM10 containing M, D, and C domains revealed the molecular details of how D and C domain regulates M domain activity. Studies have shown that ADAM10 is active only when the P domain is cleaved, however, how the P domain interacts with other domains remains unknown. To further explore the regulatory roles of the four functional domains on ADAM10 activity, we designed protein domain truncations of ADAM10 fused with various molecular tags and performed protein-protein interaction assays. The techniques used in this study include Gateway cloning, mammalian cell culture and overexpression of recombinant protein domains, GST pulldown, TR-FRET, SDS-PAGE, and Western blotting. The results showed that the P domain can interact with M, D and C domains but with a preference to M domain. This study helps to provide a better understanding on the regulation of ADAM10 activity by its functional domains. Due to the neuroprotective role of ADAM10, restoring its enzymatic activity could be beneficial. Information gained from this investigation could assist in discovery of a novel therapeutic strategy for treating AD.

An Investigation of the domain-domain interactions of A Disintegrin Metalloproteinase domain-containing protein 10 (ADAM10)

By

Richard Nwakamma

Haian Fu

Adviser

A thesis submitted to the Faculty of Emory College of Arts and Sciences
of Emory University in partial fulfillment
of the requirements of the degree of
Bachelor of Science with Honors

Chemistry

2022

Acknowledgements

I would like to thank Dr. Haian Fu for allowing me to join his lab, as this has been a wonderful experience! I would also like to acknowledge all members of the Fu lab for helping me in lab. In addition, a special shout out to Kun Qian, in the Fu lab, as she helped me out a lot with this project from the beginning to the end. I would not have been able to do this project without her help! Also, I want to say thank you to Dr. David Lynn, Dr. Monika Raj, and Professor Brenda Harmon. Thank you for your continuous support not only on this project but for the advice and encouragement you have provided me at Emory both at my time on the Atlanta and Oxford campuses. Also, I would like to thank my family and friends for their support as well. I have relied on them a lot in an effort to practice self-care especially during this year managing so many different pursuits of mine.

Table of Contents

Figures and Tables

Supplementary Figure 3: GST Pulldown assays of other ADAM10 domain constructs paired.

Supplementary Figure 4: P domain interacting with truncations of the M domain (M1 220-336) and M2 (337-459).

Introduction:

Alzheimer's disease (AD) is a neurodegenerative illness characterized by the decline in both memory and cognitive abilities as individuals age over time [3, 4]. The pathophysiology of AD is complex and not fully understood, which makes this disease more difficult to treat. It is predicted by the year 2050, AD is expected to affect 150 million people across the world [5]. In addition, new cases of AD have been shown to appear at an alarming rate of every seven seconds globally, emphasizing the rising spread of this neurological disease [6]. Currently, most prescription drugs approved by the U.S. Food and Drug Administration (FDA) are to reduce solely the symptoms of AD [7, 8]. Ongoing studies attempt to understand the mechanisms behind AD progression and to find new therapies to combat against this illness. AD pathology studies reveal that amyloid-β (Aβ) peptides and hyperphosphorylated tau, which form amyloid fibrils and neurofibrillary tangles respectively, are the hallmarks of AD [6, 7]. In 2021, the FDA provided accelerated approval for aducanumab, an immunotherapy that targets beta-amyloid and may help slow the progression of Alzheimer's, although it has not yet been shown to affect clinical symptoms or outcomes [9]. The rise of AD cases and the lack of effective treatment raise the urgent need for new and effective therapeutics to reduce the harmful neurological effects associated with AD and aid in the prevention of AD for future generations.

ADAM10 is a transmembrane protein that acts as an α-secretase to regulate the proteolytic processing of membrane bound proteins [10, 11]. ADAM10 has been associated in various biological processes and diseases including developmental signaling, neurodegenerative diseases, cancer, and inflammatory responses [12-14]. In the brain, ADAM10 is highly expressed and plays a key role in brain development where it is responsible for the shedding of several cell surface proteins such as ephrins, prion proteins, and others [13, 14]. There is evidence that suggests

ADAM10 activity is correlated with Alzheimer's disease seen in a variety of clinical studies. Cerebrospinal fluid (CSF) samples, taken from both patients with AD and age-matched controls, detected a decrease in the amount of mature or active ADAM10 in those with AD [15]. In addition, studies have shown that in patients with mild and sporadic cases of AD, there is the decreased activity of α-secretases, which is correlated with an increase in amyloid-β (Aβ) peptides [16-18]. This correlation of ADAM10 activity and the progression of AD can be explained further in ADAM10's role as a secretase (**Figure 1**).

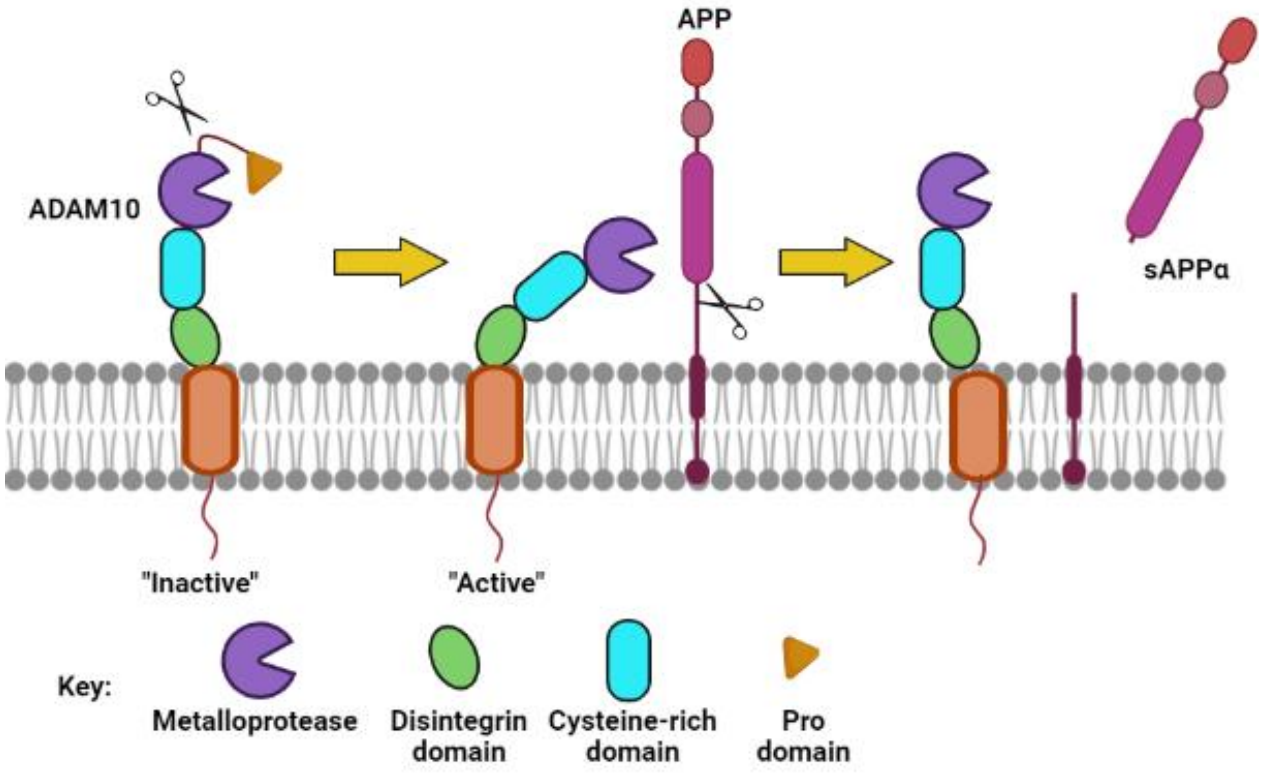

Figure 1. Non-amyloidogenic pathway of the proteolytic cleavage of APP mediated by ADAM10.

"Created with BioRender.com"

ADAM10's main role, in the context of AD, is seen in the proteolytic cleavage of the membrane protein amyloid precursor protein (APP) [19]. APP cleavage by ADAM10 generates soluble APP alpha peptides (sAPPα, **Figure 1**), which is non-neurotoxic, that in turn reduces the amount of toxic amyloid-β (Aβ) peptides generated by β- and γ-secretases [5, 20, 21]. ADAM10 activity promotes the shift to the non-amyloidogenic pathway for APP processing, whereas the amyloidogenic pathway mediated by β- and γ- secretases leads to the production of toxic Aβ peptides that later forms amyloid plaques [21, 22]. ADAM10 has been identified as the primary constitutively cleaving α-secretase responsible for cleaving APP, making it crucial for the reduction of AD pathogenesis [23, 24].

The restoration of ADAM10 activity could result in the decreased production of Aβ peptides from APP processing and prevent the progression of AD. Recent studies have shown the overexpression of ADAM10 in mice through transgenic insertion resulted in reduced Aβ peptides and plaque formation, which led to an alleviation in cognitive impairment [25]. There are currently ongoing efforts to induce ADAM10 activation by targeting key proteins and the development of small molecules as potential strategies for AD therapeutic development [26, 27]. For instance, Etazolate is a drug commonly used to treat anxiety symptoms and related disorders that has been tested in phase II AD clinical trials as a new therapeutic [28]. The mechanism of the drug is unknown, but it is thought to stimulate the GABA receptor to promote ADAM10 activity to process APP [28]. Other molecules such as protein kinase C agonist Bryostatin-1 displayed promising results in promoting ADAM10 activity in AD mouse models and is currently being tested in phase I and II clinical trials [29, 30]. Attempts have also been made to target inhibitors of ADAM10 such as the secreted frizzled related protein 1 (SFRP1). SFRP1 was found overexpressed in individuals with AD and is identified as a key therapeutic target [31]. SFRP1 can

interact with ADAM10 and is believed to interfere with the proteolytic processing of APP [5, 32]. This makes the SFRP1-ADAM10 protein-protein interaction a key target and the disruption of this interaction is another proposed strategy to restore ADAM10 activity [5, 33, 34]. This is a promising therapeutic direction but further work to enhance ADAM10 activity requires a better understanding of its structure and how other key proteins are involved in its regulation.

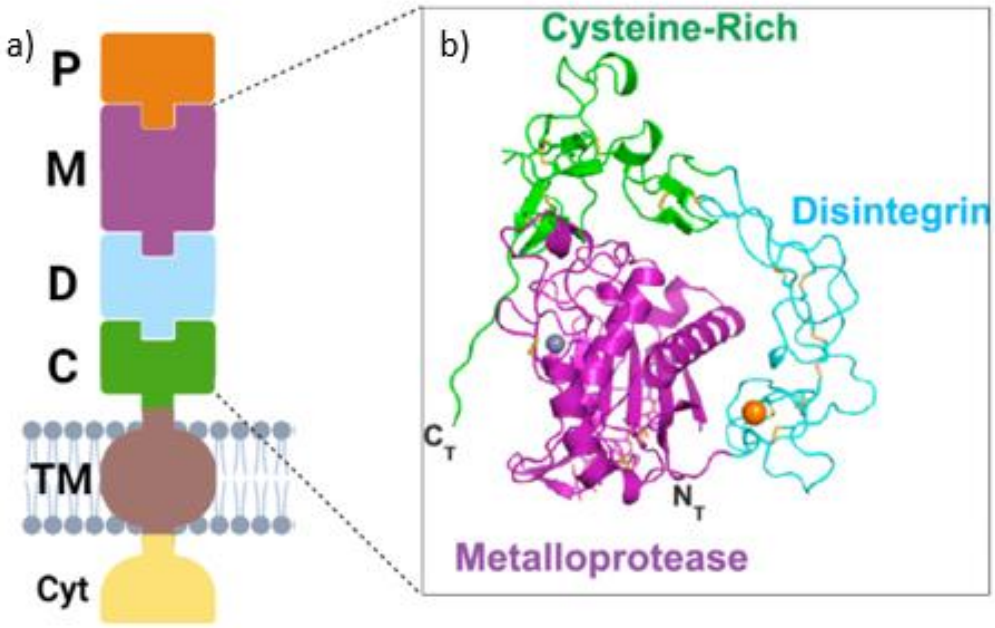

Figure 2. Structural Organization of ADAM10 a) The schematic depicts an overview of the structure of ADAM10 colored by the respective domain. P: prodomain, M: metalloprotease domain, D: disintegrin domain, C: cysteine-rich domain, TM: transmembrane domain, Cyt: cytoplasmic domain. "Created with BioRender.com". b) Crystal structure of the truncated version of ADAM10 comprised of MDC domains corresponding to the colors in Figure 2a [2].

It is important to understand in-depth how the structure of ADAM10 is affecting and regulating its function, especially if further attempts are to improve upon its activity. ADAM10

is a member of the ADAM family that have a unique organizational structure for their domains [35]. The extracellular domains present, starting from the N-terminal side, includes the pro-domain (P), metalloprotease domain (M), disintegrin domain (D), and the cysteine rich domain (C) (**Figure 2**). The crystal structure of a truncated form of ADAM10 containing the M, D, and C domains (MDC) showed how each of the domains interact with one another [2]. The main catalytic function of ADAM10 is performed by the M domain and the remaining domains are thought to play a role in the regulation of its overall activity [2, 36]. Studies revealed that only when the P domain is cleaved, ADAM10 becomes catalytically active [37] (**Figure 1**). The P domain is linked to the M domain through a proprotein convertase recognition sequence that can be cleaved by proprotein convertases [38]. Since the P domain is intrinsically disordered and difficult to obtain crystal structures, currently there is no experimental evidence on how it may interact with the other extracellular domains of ADAM10. Furthermore, it is believed that the D and C domains may play a regulatory role on the M domain seen from both the truncated structure of the MDC domains of ADAM10 (**Figure 2**) and APP shedding assays influencing the degree to which it interacts with its substrates [2, 39, 40]. Further work is needed to understand the domain-domain interactions that influence the overall ADAM10 activity.

The focus of this investigation is to explore the domain-domain interactions of ADAM10. The experimental overview is illustrated in **Figure 3**. By generating protein domain truncations of ADAM10 with various molecular tags, protein-protein interaction (PPI) assays were developed, which include Glutathione-S-transferase (GST) pulldown assay and time-resolved fluorescence energy transfer (TR-FRET) assay. These assays identified unique interactions occurred with the P domain and other domains. The findings of this study have shed more light on the structure of the P domain and further clarified the potential role the domains have on

regulating ADAM10 activity. This information could help in developing strategies to restore ADAM10 activity in AD patients, serving as a new method of treatment to combat this disease.

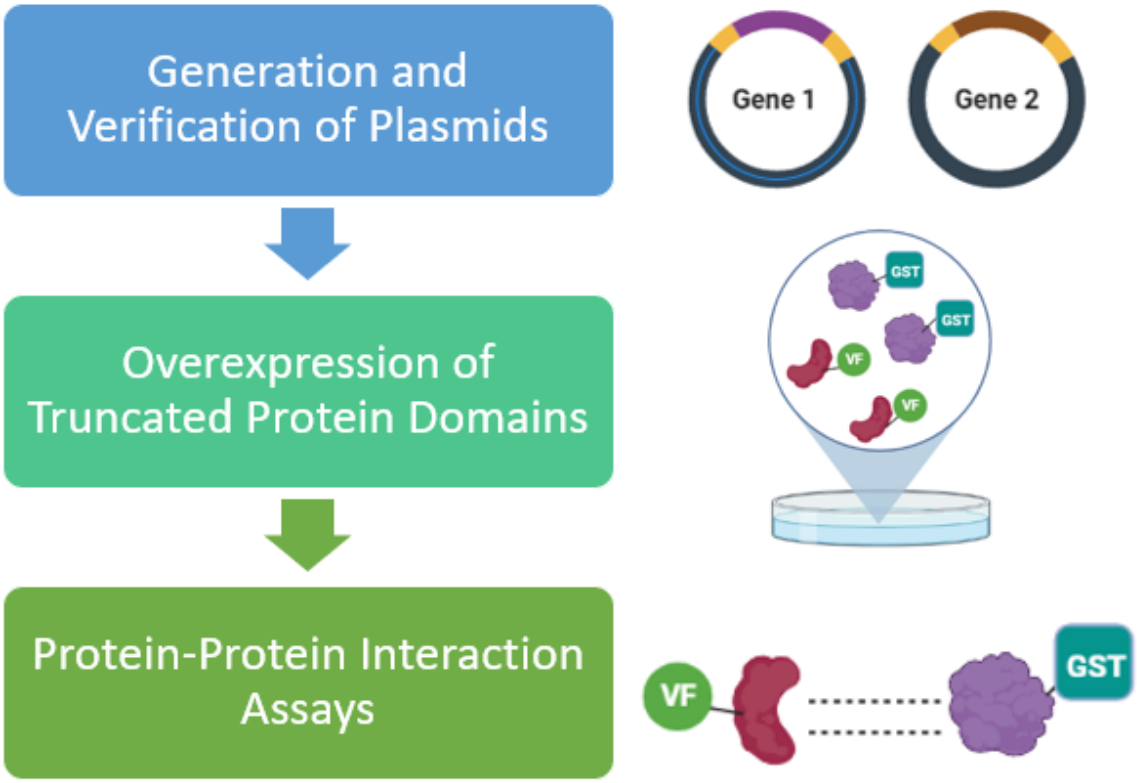

Figure 3. Experimental Overview. The schematic depicts an overview of the investigation where the generation of respective plasmids for each ADAM10 domain will first be generated, followed by overexpression in cells, and extraction of truncated protein domains for use in protein-protein interaction assays (GST pulldown and TR-FRET). "Created with BioRender.com"

Materials and Methods:

Generation and Extraction of DNA Plasmids

DNA constructs for the respective ADAM10 domain truncations were generated using PCR followed by Gateway cloning technology manual (**Supplementary Figure 1**). Plasmids were generated for the following domains, with the respective amino acid segments of ADAM10, P (1-219), M (220-459), D (455-550), C (551-672), PM (1-459), DC (455-654), and MDC (220-654). Further truncations were generated of M domains which included M1 (220-340) and M2 (340-459). The insertion gene of each truncation were generated using PCR which entailed 30 cycles of denaturation at 98°C for 30 seconds, annealing at 60°C for 30 seconds, extension of DNA at 72°C for 40 seconds, and final extension at 72°C for 10 minutes. All primers used are displayed in **Supplementary Table 1** for reference.

All PCR products underwent Gateway cloning (Invitrogen) to generate fused-protein plasmids with Venus Flag (VF) tag or Glutathione-S-transferase (GST) tag incorporated. Entry vectors (pDONR221) were generated by the BP reaction and then transformed into TOP10 competent E. coli cells and inoculated to promote growth. All plasmids were extracted through miniprep and verified using agarose gel electrophoresis. pDONR plasmids underwent LR reactions to generate destination vectors (pDEST). These plasmids had genes incorporated for the addition of molecular tags VF and GST and followed a similar protocol for pDONR for extraction and verification. All plasmids were extracted using QIAprep Spin Miniprep kits and ZymoPURE Plasmid Maxiprep kits (Zymo Research, catalog no. D4203).

Verification of ADAM10 Plasmids

All ADAM10 domain constructs were further verified using restriction enzyme digestion followed by agarose gel electrophoresis. The setup for the digestion included preparation of an enzyme digestion buffer with restriction enzyme Bsp1407I dissolved in FastDigest Green Buffer

(FastDigest Bsp1407I, Catalog no. FD0933) and all plasmids used were diluted to $100\frac{ng}{\mu L}$ in a 6 µL total solution. The solutions were boiled in a water bath at 37°C for 30 minutes. All samples then underwent agarose gel electrophoresis for identification. A 1% agarose gel was prepared, and an electrophoresis chamber was prepared with 1X TBE buffer, and the following suspensions were inserted into the wells: 6 µL of the digested plasmid solution and 6 µL of 1 Kb DNA ladder. The gel ran at a voltage of 150 for 20 minutes. The gel's image was taken by the Bio Rad ChemiDoc Imaging system for analysis. Fragments were generated for some ADAM10 plasmids using the restriction enzyme digestion. The NEBcutter program (New England BioLabs Inc.) was used to identify enzyme digestion sites along with the expected number of fragments and sizes for all plasmids. Constructs with expected insertion gene size were further outsourced for verification by Sanger sequencing at Genewiz.

Cell Culturing and Transfection of HEK293T Cells

A human kidney cell line, HEK293T, is used for overexpression of the plasmids. Dulbecco's Modified Eagle's Medium (DMEM; Corning, catalog. no. 10-013-CV) was used for cell culture, which contained 4.5 g/L glucose, L-glutamine, and sodium pyruvate with 10% fetal bovine serum (FBS) and a 1% antibiotic mixture of penicillin/streptomycin added (CellGro, catalog. no. 30-002-CI). HEK293T cells were maintained in a cell incubator at 37 ^{o}C with 5% CO_2. In a typical transfection experiment, HEK293T cells grown to 60%-70% confluency in a 6-well plate were transfected with VF and GST tagged plasmids corresponding to specific ADAM10 domain truncations, with a total plasmid amount of 3 µg. Transfection was performed using 1 mg/ml polyethyleneimine (PEI; Polysciences, Inc., catalog no. 23966) as the transfection reagent in a standard ratio of 3 µg of PEI to 1 µg of DNA plasmid. The efficiency of transfection

was observed qualitatively using the ZOE Fluorescent Cell Imager by the fluorescence emitted by VF-tagged constructs, and further detected by western blotting using tag specific antibodies.

GST Pulldown Assay

HEK293T cells were co-transfected with respective GST and VF-tagged ADAM10 domain constructs and were incubated for 48 hours. Harvested cell pellets from a single 6-well were lysed using 200 µL of 0.5% Triton X-100 Lysis buffer (20 mM Tris-HCl, 150 mM NaCl, 5% glycerol, 0.5% Triton X-100, and 2 mM EDTA) with the addition of protease inhibitor (catalog. no. P8340) and phosphatase inhibitor cocktail (catalog. no. P0044 and P5726) followed by sonication for 10s and centrifugation for 10 min. at 13,200 r.p.m. at 4°C. All cell lysates were collected and incubated with glutathione-conjugated beads (GE Healthcare, catalog no. 17–0756-05) for 2 hours rotating at 4°C. After incubation, all beads were washed 3 times using the lysis buffer and were eluted by boiling for 3 minutes in sodium dodecyl sulfate (SDS)-polyacrylamide gel electrophoresis (SDS-PAGE) loading buffer and stored at -20°C. All samples were analyzed using Western Blotting and respective antibodies.

Antibodies

The mouse Monoclonal Anti-Flag M2- Peroxidase (HRP) antibody (catalog. no. A8592), rabbit polyclonal anti-Glutathione-S-Transferase (GST)- Peroxidase Conjugate antibody (catalog. no. A7340), and mouse monoclonal anti-Glutathione-S-Transferase (GST)- antibody (catalog. no. G1160), were purchased from Sigma-Aldrich. The Peroxidase AffiniPure goat anti-rabbit IgG (H + L) secondary antibody (catalog. no. 111-035-003) and the Peroxidase AffiniPure goat anti-mouse IgG (H + L) secondary antibody (catalog. no. 111-035-003) were purchased from Jackson ImmunoResearch Inc. The Tb cryptate-conjugated monoclonal anti-GST antibody

(anti-GST-Tb, catalog. no. 61GSTTLB) and d2-conjugated anti-Flag antibody (anti-Flag-d2, catalog. no. 61FG2DLB) were purchased from Cisbio Bioassays (Bedford, MA).

Western Blotting

All protein samples were separated using sodium dodecyl sulfate polyacrylamide gel electrophoresis (SDS-PAGE). 10% gels were used and allowed to run for 1 hr. at 150V. Proteins on the gel were transferred onto a nitrocellulose filter membrane at 100V for 2 hours at 4°C. All membranes were blocked in 5% nonfat dry milk dissolved in TBST buffer (20 mM Tris-base, 150 mM NaCl, and 0.05% Tween 20) for 30 min. All membranes were then incubated in respective primary antibody solutions overnight at 4°C while secondary antibodies were incubated for 1 hour at room temperature. All membranes were washed 3 times for at least 3 minutes each time in TBST buffer. SuperSignal West Pico PLUS Chemiluminescent Substrates (Thermo, catalog no. 34580) or Dura Extended Duration Substrates (Thermo, catalog no. 34076) were used for detection. All Western blot imaging was performed using a ChemiDoc imaging system (Bio-Rad).

TR-FRET Assay

All TR-FRET assays were performed using the lysates of HEK 293T cells expressing VF-tagged and GST-tagged ADAM10 domain constructs in 384 black well plates. Cells had previously underwent transfection and after 48 hours cell lysates were extracted. Assay buffer contained 20 mM Tris-HCl, pH 7.0, 50 mM NaCl, and 0.01% nonidet P-40 (NP-40). Respective GST-Terbium (Tb) and Flag-d2-conjugated antibodies were used for GST and VF tagged constructs, respectively. For each well, the total volume was 20 µL where 10 µL of cell lysates underwent a serial dilution using the reaction buffer, then 10 µL of an antibody mixture was added to reach final ratio of 1:1000 GST-Tb and 1:500 Flag-d2. All plates were centrifuged at

1000 r.p.m. for 1 min. and were left to incubate for more than 2 hours or overnight at 4 °C. The TR-FRET signals were measured using the BMG Labtech PHERAstar FSX plate reader.

Results:

Construction and Verification of Plasmids

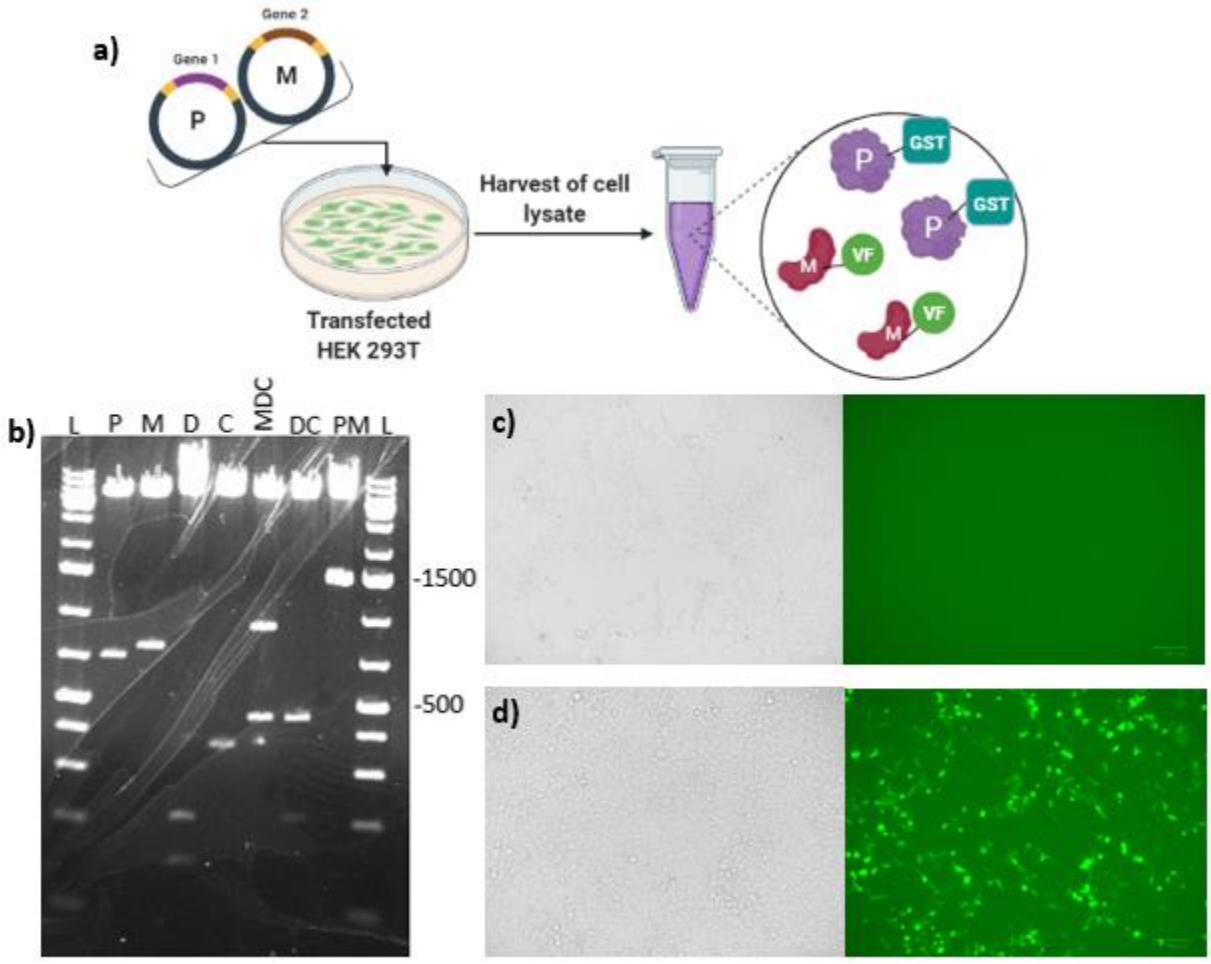

Figure 4. Generation and verification of ADAM10 domain plasmids by gel electrophoresis followed by overexpression in HEK293T cells. a) Illustration depicting the co-transfection of plasmids for two respective protein domains and the cell lysate collected with VF and GST tagged fusion proteins [41]. b) Image of an agarose gel from DNA electrophoresis depicting the plasmids of pDEST vectors for respective VF tagged protein domains after Bsp1407I enzyme digestion. All plasmids are labeled by their respective domain truncation (P, M, D, etc.) and

DNA ladders are represented by L. c) Image depicting transfected HEK293T cells after incubation with an empty plasmid (pcDNA) under a brightfield view on left and green-fluorescent channel view on right. d) Transfected HEK293T cells are displayed after transfection with VF-PM plasmid for 2 days under brightfield (left) and green-fluorescent channel (right).

ADAM10 domain truncation plasmids for mammalian cell expression were generated for each respective domain using Gateway cloning (**Supplementary Figure 1**). All plasmids had a GST or VF tag attached with a respective orientation (N-terminal or C-terminal) and were purified from Top10 cell culture (E. Coli). Plasmids were then verified using agarose gel electrophoresis, indicated by the expected base pair size of the respective plasmid. The exact sizes for each domain truncation for P, M, D, C, MDC, DC, and PM are respectively 657bp, 720bp, 288bp, 366bp, 1320bp, 600bp, and 1377bp. The observed base pair sizes of the VF-tagged plasmids of P, M, D, C, MDC, DC, and PM generated are approximately 700bp (P and M), 200bp, 400bp, 1000bp, 500bp, and 1500bp, respectively (**Figure 4b**). The observed sizes of each domain on the DNA gel reflected their expected sizes. Fragments for respective plasmids are seen in the gel for D, MDC, and DC (**Figure 4b)**. Respective fragment sizes sum up to the observed sizes that were mentioned previously. The plasmids were further verified using a Sanger sequencing service, the results were aligned with their known sequences and matched (data not shown). Verified expression plasmids were transfected in HEK293T cells for tag fused protein expression (**Figure 4a**). The efficiency of transfection and protein expression can be seen by the emitted green fluorescence from HEK293T cells transfected with VF tagged plasmid, comparing to the brightfield (**Figure 4d**). Cells transfected with an empty plasmid (pcDNA) with no expression of VF are expected to show no fluorescence (**Figure 4c**). The expression of both

VF-tagged and GST-tagged proteins are also confirmed by Western Blotting of the respective whole cell lysates transfected with the plasmid (data not shown).

Experimental Design of TR-FRET and GST Pulldown Assays

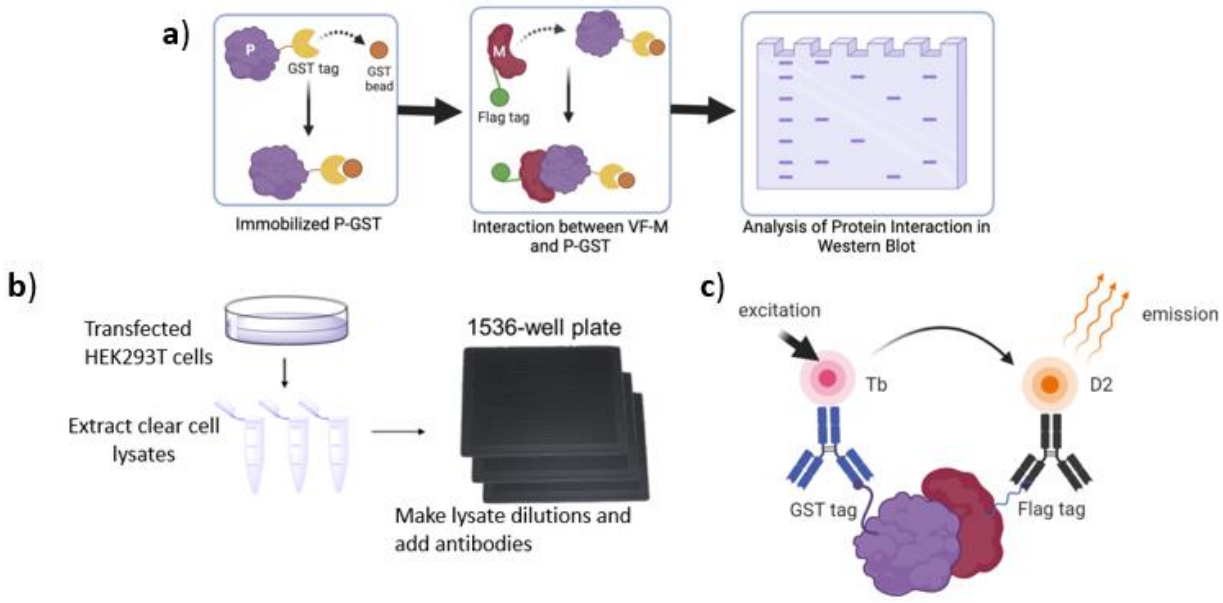

Figure 5. Illustration depicting workflow of GST Pulldown and TR-FRET Assays. a) Schematic depicting the setup of the GST pulldown assay using GST-tagged P domain and VF-tagged M domain plasmids. In whole cell lysates, overexpressed GST-tagged P domain is captured by glutathione beads, which is interacting with the VF-tagged M domain [42] b) Illustration describing the workflow of the TR-FRET assay. "Created with BioRender.com" c) Schematic of the design of the TR-FRET assay for detecting interactions between truncated ADAM10 domains [43]. Anti-GST-Tb antibody serves as the TR-FRET donor and the anti-Flag-D2 serves as the acceptor. When the donor and acceptor are close enough with <10 nm in distance, the FRET signal is emitted to indicate an interaction between the two target proteins.

HEK293T cells were overexpressed with two respective ADAM10 domain truncations though a co-transfection using two distinct plasmids. Cell lysates were extracted and used to perform GST pulldowns and TR-FRET assays to identify PPIs (**Figure 5**). The GST pulldown assay captures the GST tagged protein with glutathione resin from the whole cell lysate, while the interacting proteins are also pulled down on the resin (**Figure 5a**). Multiple domains were paired together and tested to ensure each respective domain could interact with all possible combinations. A list of all the various combinations of ADAM10 domains tested is summarized in **Supplementary Table 2**. The TR-FRET assay is used to verify interactions identified from GST pulldowns. Respective antibodies were added to whole cell lysates that serve as the donor (Anti-GST-Tb) and acceptor (anti-Flag-D2), which bind to respective GST or VF- tagged ADAM10 domains (**Figure 5b**). When the donor and acceptor are in proximity, which is mediated by the ADAM10 domain-domain interactions, the FRET signal turns on, indicating a PPI (**Figure 5c**). These two assays use different approaches to identify PPIs, but the utility of incorporating both helps to circumvent for any experimental artifacts such as variation in the intensity of bands (GST pulldown) or fluorescent interferences (TR-FRET). Additionally, for both techniques, the direction of fusion tags was switched to test for all possible combinations, taken into consideration the effect the tag orientation may have on the binding of the ADAM10 domains.

Identifying Interactions of the Pro domain with truncated ADAM10 domains

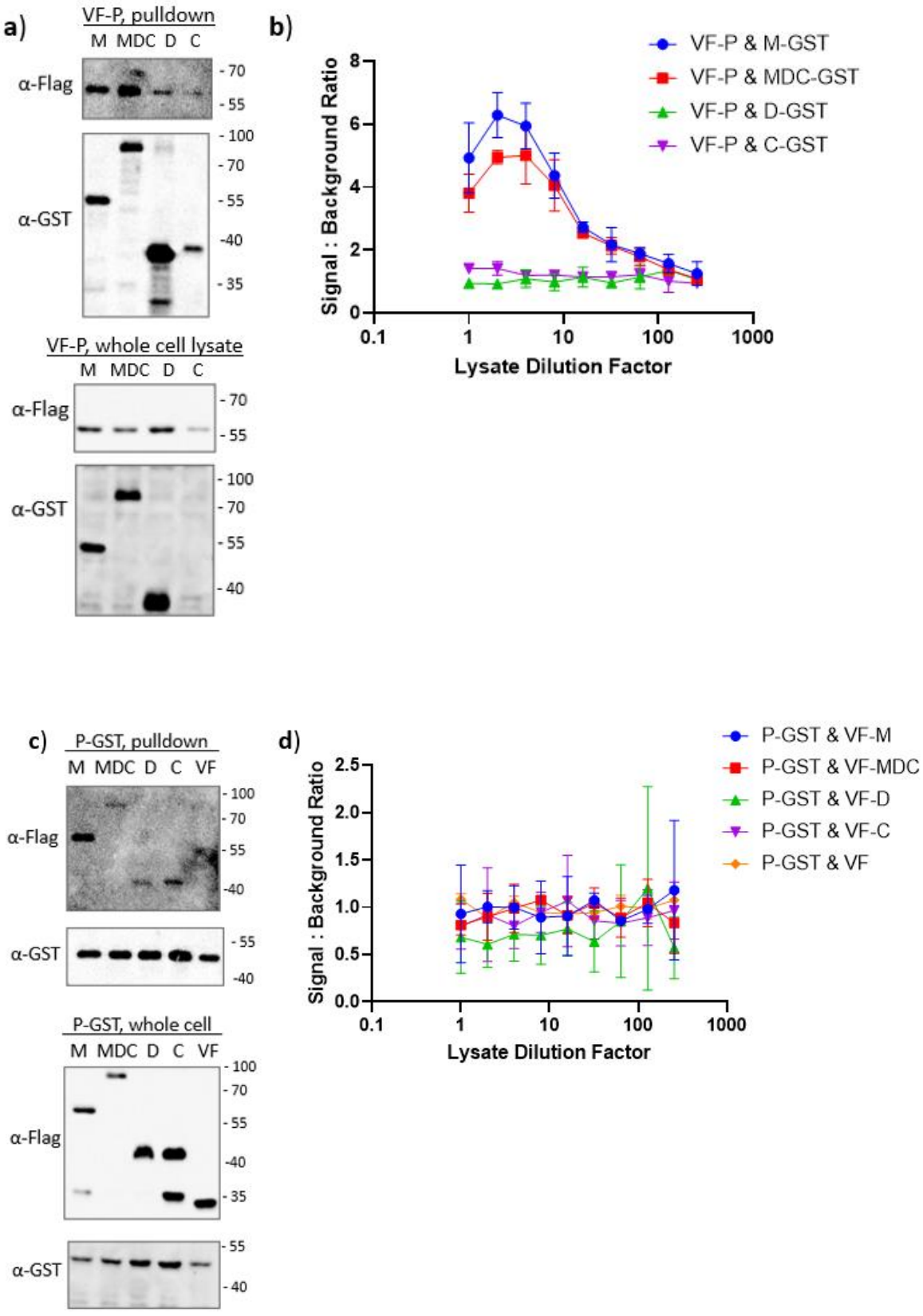

Figure 6. GST Pulldown and TR-FRET of ADAM 10 P domain constructs interacting with M, MDC, D, and C domains. Molecular weight indicated by the protein ladder is marked on the right side of each blot. **a)** GST pulldown testing the interaction of N-terminal VF-tagged P domain construct (VF-P) with respectively C-terminal GST-tagged M, MDC, D, and C domain constructs. **b)** TR-FRET signals displayed of the interactions between VF-P and (M, MDC, D, and C)-GST. All interactions tested consisted of 2 trials and the signals displayed represent the mean and standard deviation. **c)** GST pulldown testing the interaction of C-terminal GST-tagged P domain construct (P-GST) with respectively N-terminal VF tagged M, MDC, D, and C constructs. VF vector without protein fusion was used as a negative control for each experimental setup. **d)** TR-FRET signals displayed of the interactions between P-GST and VF-(M, MDC, D, and C). All interactions tested consisted of 2 trials and the signals displayed represent the mean and standard deviation.

GST pulldowns were performed in tandem with TR-FRET assays using the same plasmid concentrations in transfection. N-terminal VF-tagged P domain constructs (VF-P) showed interactions with all respective C-terminal GST-tagged domain truncations of M, MDC, D, and C (**Figure 6a**). C-terminal GST-tagged P domain constructs (P-GST) also displayed interactions with the same pairs in N-terminal VF tagged fusions. (**Figure 6c**). The assay is repeated by changing plasmid concentrations for transfection, which changes the level of protein expression in whole cell lysates. In **Supplementary Figure 2a**, C-terminal GST-tagged P domain (P-GST) interacted with all respective N-terminal VF-tagged M, D, C, DC, and MDC domains. Overall, the signal reflecting interactions between P domain and M domain is the most intense (VF-P pulldown by M-GST in **Figure 6a** and VF-M pulldown by P-GST in **Figure 6c**). In the pulldown blot **Figure 6a**, the band intensity of P and MDC interaction is comparable to P and M

interaction, however, in the pulldown blot of **Figure 6c,** P and MDC interaction seems weaker, which could be due to the lower expression level of VF-MDC in the whole cell lysate. The interaction of P with D and C domains were not as intense compared to interaction with M.

For the TR-FRET assays, VF-P domain constructs showed interactions with GST-tagged domain truncations of M and MDC, which has been repeated in two independent experiments (**Figure 6b and Supplementary Figure 2b**). This distinction is the most significant as the dilution factor of cell lysate is between 4 and 8 and the signal-to-background ratio is greater than 4. However, the signal-to-background ratio of VF-P and GST tagged D and C domains are approximately 1, indicating no TR-FRET signal for these pairs (**Figure 6b and Supplementary Figure 2b**). When tags were switched testing interactions of P-GST with VF- (M, MDC, D, and C), the signals were not distinct from one another, and they were close to the background (**Figure 6d**). This is possibly due to the mechanism of the TR-FRET signal generation. The TR-FRET signal emits when the distance of the donor and acceptor is less than 10 nm **(Figure 5c)**, while the size of the tags (VF is 26 kD and GST is 27 kD) and their orientations (N-terminal fusion or C-terminal fusion) could affect the distance between the donor and acceptor molecules conjugated on the specific antibodies.

From both the GST pulldown and TR-FRET assays, it can be confirmed that P interacts with M and MDC domains. These interactions occurred in both GST pulldowns (**Figures 6a, 6c, and Supplementary Figure 2a**) and TR-FRET assays (**Figures 6b and Supplementary Figure 2b**). This led to further attempts to narrow down the binding interaction of the P and M domain, which involved generating smaller truncations of each respective domain and perform GST pulldowns and TR-FRET assays. Some preliminary results can be seen in **Supplementary**

Figure 4 as conditions of the experiment would need to be further optimized to increase protein expression level.

Identifying Interactions of the M and PM domains with truncated ADAM10 domains

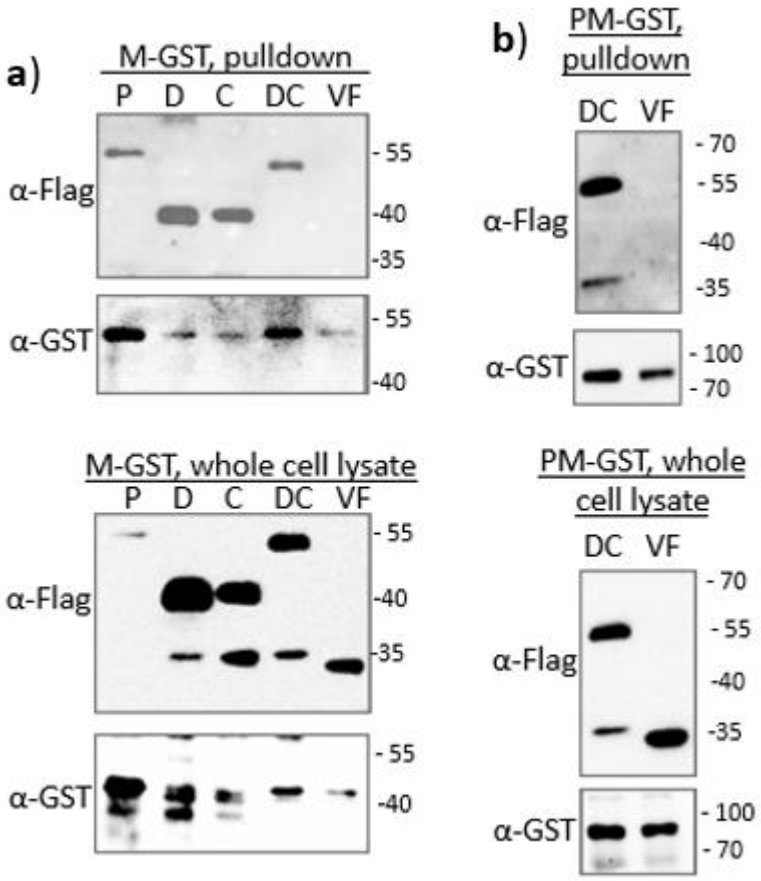

Figure 7. GST Pulldown Assay of M and PM domain interacting with other ADAM10 domain constructs. a) Interaction of C-terminal GST-tagged M domain construct (M-GST) with respectively N-terminal VF tagged P, D, C, and DC constructs. b) Interaction of C-terminal GST-tagged PM domain construct (PM-GST) with respectively N-terminal VF tagged DC constructs. VF vector without protein fusion was used as a negative control. Molecular weight indicated by the protein ladder is marked on the right side of each blot.

Additional GST pulldown assays were performed to identify interactions occurring between other ADAM10 domain truncations. In **Figure 7a**, C-terminal GST-tagged M domain (M-GST) interacted with all respective N-terminal VF-tagged P, D, C, and DC domains. In **Figure 7b**, C-terminal GST-tagged PM domain (PM-GST) interacted with VF-tagged DC domain. A list of all the combinations of ADAM10 domains tested is summarized in **Supplementary Table 2**. Additional pulldown results are shown in **Supplementary Figure 3**, as those not specifically mentioned either showed no expression in whole cell lysates, or the molecular weight of the corresponding fused-protein domain was inaccurate.

Discussion:

ADAM10 plays a critical role in promoting the non-amyloidogenic pathway and reduces the amount of toxic amyloid-β (Aβ) peptides associated with AD [44, 45]. This has led to attempts to increase ADAM10 activity serving as a new potential therapy in combatting against AD [12, 46, 47]. The structure of the full-length version of ADAM10 is not completely understood, while it is crucial in the understanding of how its extracellular activity is being regulated. Previous work indicated that the P, D, and C domains of ADAM10 play a role in regulating the activity of the M domain [48-50]. The P domain acts as a switch turning on and off the protease activity of ADAM10, but how it interacts with other domains remains unclear [48]. In this study, we aim to dissect the domain-domain interactions of ADAM10's extracellular component and hope to fill in the gap of knowledge on how these domains could participate in regulating ADAM10 activity. Findings from this study provide a basis to better understand the structural regulation of ADAM10 and help in restoring the neuroprotective role of ADAM10 to serve as a new therapeutic strategy to treat AD.

This investigation explored the binding interactions of the extracellular domains of ADAM10. By creating expression plasmids of domain truncations, various domain pairs were tested with one another in cell lysate-based protein-protein interaction assays such as GST pulldown assay and TR-FRET assay.

The GST pulldown assay isolates protein-protein interactions from the whole cell lysates expressing the proteins of interest (**Figure 5a**). We identified various domain-domain interactions led by the M domain and P domain. The M domain has already been displayed to interact with the D and C domains in the crystal structure of MDC [2, 48]. It is thought to play an autoinhibitory role as this domain truncation partially occludes the active site of the M domain

(**Figure 2**) [2, 51]. This further suggests that the D and C domains interact with the M domain to regulate its affinity to substrates such as APP [2, 36]. The results of our work displayed that the M domain interacts with D, C, and DC domains, which further validated previous findings (**Figure 7a**). We discovered that P domain interacts with all the other various domains including M, D, C, DC, and MDC. GST pulldown results of N terminal VF-P displayed interactions with C-terminal GST constructs of M, MDC, D, and C domains, while signal intensities of D and C are weaker (**Figure 6a**). For pulldowns with C-terminal P-GST, interactions were also seen with N terminal VF tagged M, MDC, D, and C with variation in the signal intensities (**Figure 6c and Supplementary Figure 2a**). One limitation with this assay is that the data analysis is primarily qualitative. The intensity of the bands in western blots serves to identify interactions that are occurring but is not the direct indication of the strength or affinity of the interactions being observed, especially considering the variations in protein expression level in the whole cell lysate, and variations in the efficiency of GST pulldown toward different domain constructs.

TR-FRET assay uses a different readout to detect PPIs and helped to verify interactions identified using GST pulldown assays. From the results, it is observed that the P domain interacted with both the M and MDC domains, shown respectively from the interactions of N terminal VF-P with C terminal M-GST and MDC-GST (**Figures 6b and Supplementary Figure 2b**). However, interactions of the P domain (VF-P) with the D (D-GST) and C (C-GST) domains not detected (**Figures 6b and Supplementary Figure 2b**). Based on the principal of FRET, we expect that the orientation of the tag fusion could have a significant influence on the FRET signal, as it is dependent on the position of the donor and acceptor that are conjugated to the tag specific antibodies. When testing interactions of N terminal VF-P and C terminal M and MDC constructs, interactions were seen as previously mentioned (**Figures 6b and Supplementary**

Figure 2b) and was consistent with the GST pulldown results. When tags were switched using C-terminal P-GST with N terminal VF tagged M and MDC, signals were close to the background (**figure 6d**). The size of the tag could also play a role. The GST and VF tags added are respectively 26kDa and 28kDa, while P, M, D, and C are respectively 24kDa, 27kDa, 5kDa, and 6kDa. The effect of adding a large tag could be more significant when the domains are small, such as in D and C. This could explain why interactions between P with D and C were not displayed in TR-FRET assays (**Figures 6b and Supplementary Figure 2b**) as they were shown weakly in the GST pulldowns (**Figures 6a, 6c, and Supplementary Figure 2a**).

Combining the findings from GST pulldown assay and TR-FRET assay, we find that the signals reflecting interaction of P domain with M domain or MDC domain is more significant than the interaction of P domain with D domain or C domain. It also suggests that the interaction between P domain and MDC domains could be mediated primarily by the M domain. The results support the predicted structure of ADAM10 using Alphafold. The predicted P domain is seen to have a binding interface with the M domain; the image shows an α-helical structure of the P domain in silver having contact with the M domain in purple (**Figure 8a**). The D domain in blue has a loop-like region being in contact with a loop-like structure in silver of the P domain (**Figure 8b**). The C domain in green seems to have a small interface with the P domain in silver through similar loop-like regions (**Figure 8c**). Although there is a big helical portion in silver of the P domain that extends away from the C domain (**Figure 8c**). The backside of the P domain is shown to have some contact with both the D domain and C domain, but there is no significant contact being depicted with the D and C domains (**Figures 8b and 8c**). Overall, the structure showed that the P domain presented a major interaction interface with the M domain, indicated by an α-helical region in the P domain and less with the D and C domains (**Figure 8**).

a)

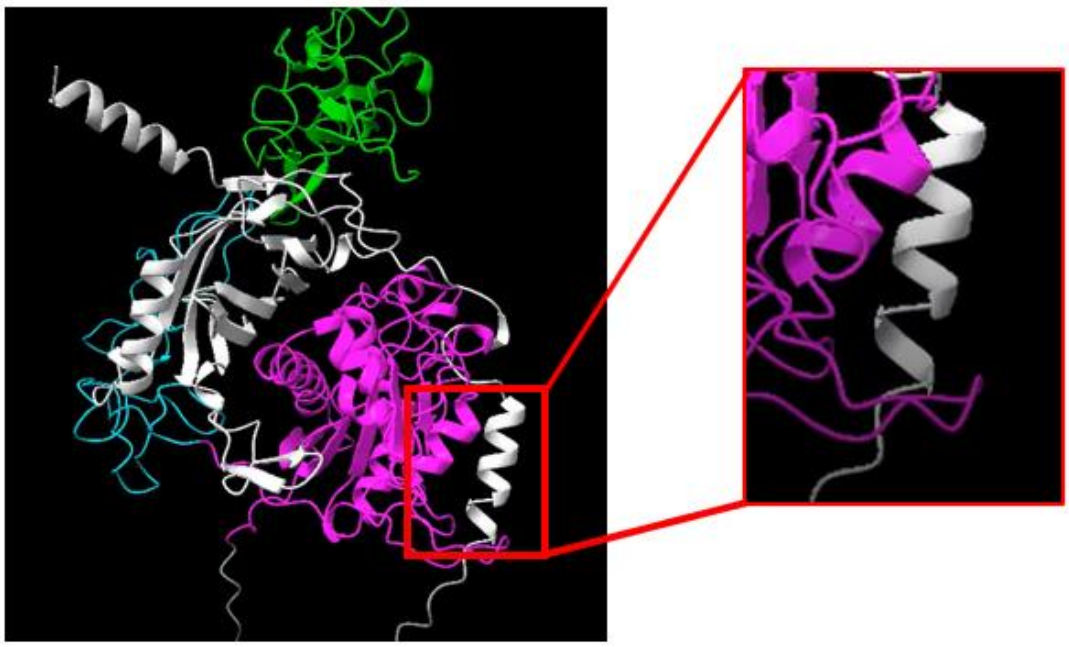

b)

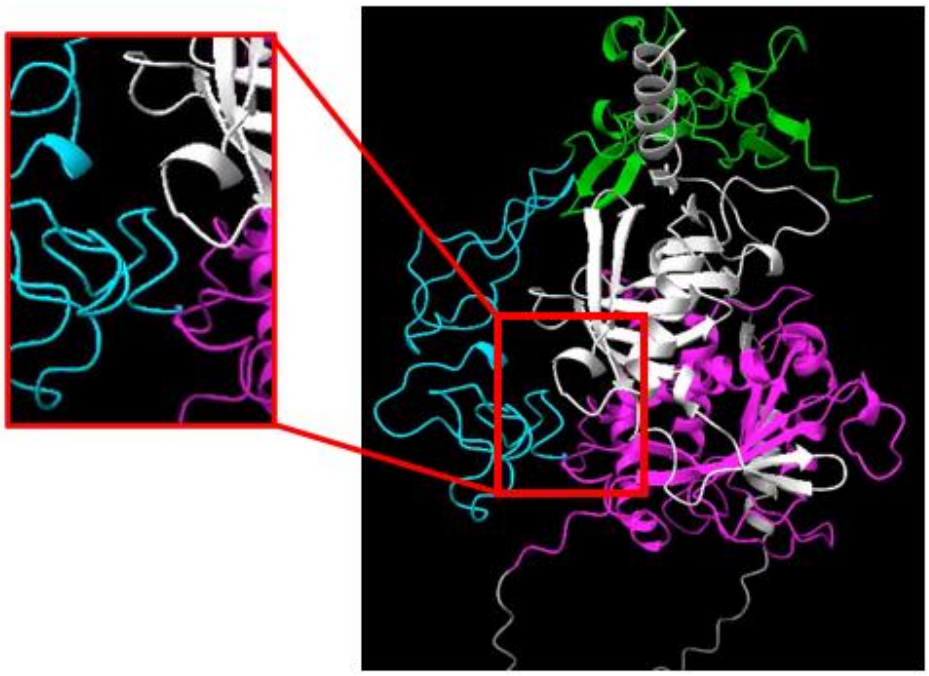

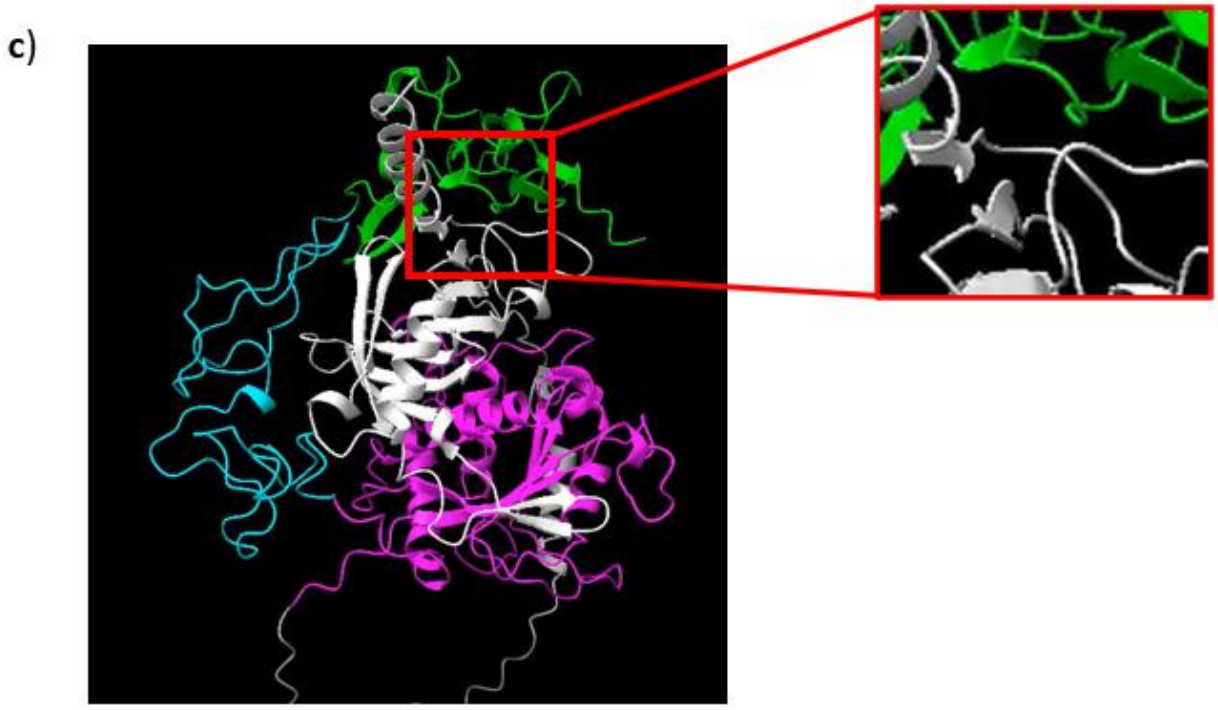

Figure 8. Alphafold Predicted Structures of Full Length ADAM10. M domain is depicted in purple, D domain in blue, C domain in green, and predicted P domain shown in grey. **Figures 8a-8c** depict rotated views of ADAM10 with magnified portions of the predicted binding interfaces of P and M (**Figure 8a**), P and D (**Figure 8b**), and P and C (**Figure 8c**).

Future Directions and Conclusions:

The findings from this work identified that among the extracellular domains of ADAM10, the P domain interacts primarily with the M domain, and supports previous work in the crystal structure of a truncated ADAM10 that the M domain interacts with both the D and C domains. This work helped to shed new light on the interactions of the P domain with M, D and C domains. Studies are being conducted to map the binding surface of the P and M domain to understand which specific regions are key to this interaction. This involved generating new domain truncations and testing in both GST pulldown and TR-FRET assays. Further studies will involve identifying the key amino acid residues associated with the domain-domain interactions of ADAM10. We propose to use a molecular docking tool to analyze the domain-domain interaction interfaces, identify potential amino acids that are crucial to the binding, and generate site-specifically mutated domain constructs to test in PPI assays. Other studies would also involve using purified protein domains for biophysical direct binding assays to determine the binding affinities of the interactions.

Ultimately, understanding the structural regulation of ADAM10's extracellular domain provides a basis to develop novel methods to target ADAM10 activity, such as the discovery of small molecules that restore its neuroprotective activity, which could potentially lead to a new therapeutic strategy to treat patients diagnosed with Alzheimer's disease.

Supplemental Information:

Supplementary Table 1. Primers used in the Generation of ADAM10 Domain Truncations using PCR

ADAM 10 Domains (amino acid designations)	Molecular Weight (kDa)	Forward (F) and Reverse (R) Primers Used
Pro domain (P) (1-213 or 1-219)	25	F:gggg aca agt ttg tac aaa aaa gca ggc ttc gaaggagata ga accatg gcc GTGTTGCTGAGAGTGTTAATTCTGC Rp219: gggg ac cac ttt gta caa gaa agc tgg gtt TTTTTCAGCTGAAGTTGTACG Rp213: gggg ac cac ttt gta caa gaa agc tgg gtt ACGTTTTTTCCTCAGAAGTTC
Metalloprotease domain (M) (220-459)	27	F: gggg aca agt ttg tac aaa aaa gca ggc ttc gaaggagata ga accatg gcc ACTTGTCAGCTTTATATTCAGACTG R: gggg ac cac ttt gta caa gaa agc tgg gtt AATAGGTTGGCCAGATTCAAC
M1 (220-336)	13	F: gggg aca agt ttg tac aaa aaa gca ggc ttc gaaggagata ga accatg gcc ACTTGTCAGCTTTATATTCAGACTG R:gggg ac cac ttt gta caa gaa agc tgg gtt AGGTGCTCCAACCCAAGCCAG
M2 (337-459)	13	F:gggg aca agt ttg tac aaa aaa gca ggc ttc gaaggagata g a accatg gcc TCAGGAAGCTCTGGAGGAATATG R: gggg ac cac ttt gta caa gaa agc tgg gtt AATAGGTTGGCCAGATTCAAC
Disintegrin domain (D) (455-550)	5	F:gggg aca agt ttg tac aaa aaa gca ggc ttc gaaggagata g a accatg gcc GGCCAACCTATTTGTGGAAATGG R: gggg ac cac ttt gta caa gaa agc tgg gtt TGGTTTAGGGTCAGATGCTG
Cysteine -rich domain (C) (551-672)	6	F:gggg aca agt ttg tac aaa aaa gca ggc ttc gaaggagata g a accatg gcc AACTTCACAGACTGTAATAGG R: gggg ac cac ttt gta caa gaa agc tgg gtt TAGAGGACCATCAGCATCTAC
PM (1-459)	52	F:gggg aca agt ttg tac aaa aaa gca ggc ttc gaaggagata ga accatg gcc GTGTTGCTGAGAGTGTTAATTCTGC R: gggg ac cac ttt gta caa gaa agc tgg gtt AATAGGTTGGCCAGATTCAAC

MDC (220-654)	48	F: gggg aca agt ttg tac aaa aaa gca ggc ttc gaaggagata ga accatg gcc ACTTGTCAGCTTTATATTCAGACTG R: gggg ac cac ttt gta caa gaa agc tgg gtt TAGAGGACCATCAGCATCTAC
DC (455-654)	11	F:gggg aca agt ttg tac aaa aaa gca ggc ttc gaaggagata g a accatg gcc GGCCAACCTATTTGTGGAAATGG R: gggg ac cac ttt gta caa gaa agc tgg gtt TAGAGGACCATCAGCATCTAC

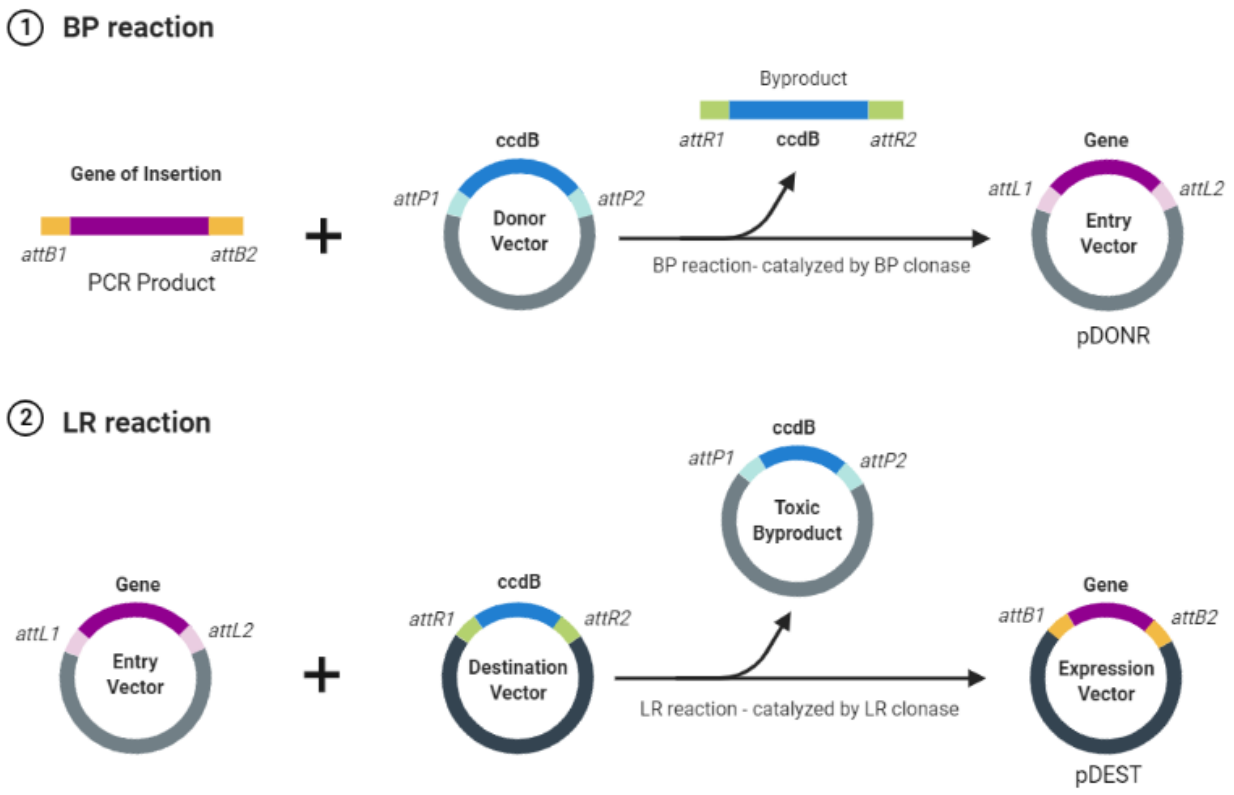

Supplementary Figure 1. Overview of Gateway Cloning Illustration depicting Gateway Cloning the process used to generate GST or VF tagged ADAM10 domain constructs [1]. PCR was used to generate the initial gene of insertion to encode the ADAM10 domain truncation. BP reaction was used to insert the gene into a donor vector generating an entry vector pDONR 221. All pDONR vectors were then transformed into TOP10 E. Coli and later extracted to for use in LR reactions. The LR reaction allowed for the transfer of the gene of interest into a destination vector creating an expression vector (pDEST) that would also be encoded to express a GST or VF tag.

Supplementary Table 2. ADAM10 Domain Pairs assigned in GST Pulldowns

C-terminal GST tagged domains (domain- GST)	N-terminal VF tagged domains (VF-domain)
P-GST	VF-M
	VF-D
	VF-C
	VF-DC
	VF-MDC
	VF
M-GST	VF-P
	VF-D
	VF-C
	VF-DC
	VF
PM-GST	VF-D
	VF-C
	VF-DC
	VF
C-GST	VF-P
	VF-M
	VF-D
D-GST	VF-P
	VF-PM
	VF-M
	VF-C
	VF

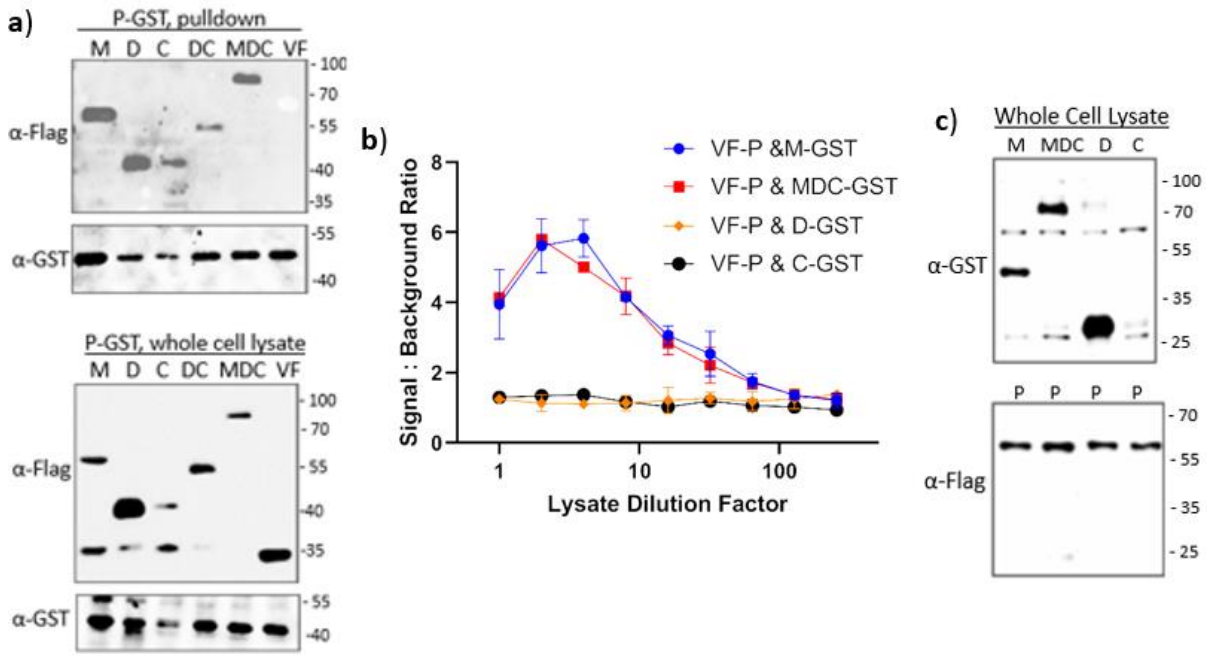

Supplementary Figure 2. TR-FRET and Optimized GST Pulldown assay of ADAM 10 P domain constructs interacting with M, D, C, DC, and MDC domains. Molecular weight indicated by the protein ladder is marked on the right side of each Blot. **a)** GST pulldown testing the interaction of C-terminal GST-tagged P domain construct (P-GST) with respectively N-terminal VF-tagged M, D, C, DC, and MDC constructs (VF-M, VF-D, VF-C, VF-DC, and VF-MDC). VF vector without protein fusion was used as a negative control for each experimental set up. **b)** TR-FRET signals displayed of the interactions between VF-P and (M, MDC, D, and C)-GST. All interactions tested consisted of 2 trials and the signals displayed represent the mean and standard deviation. **c)** Whole cell lysates were collected to measure protein expression for all respective fused domains being tested in TR-FRET.

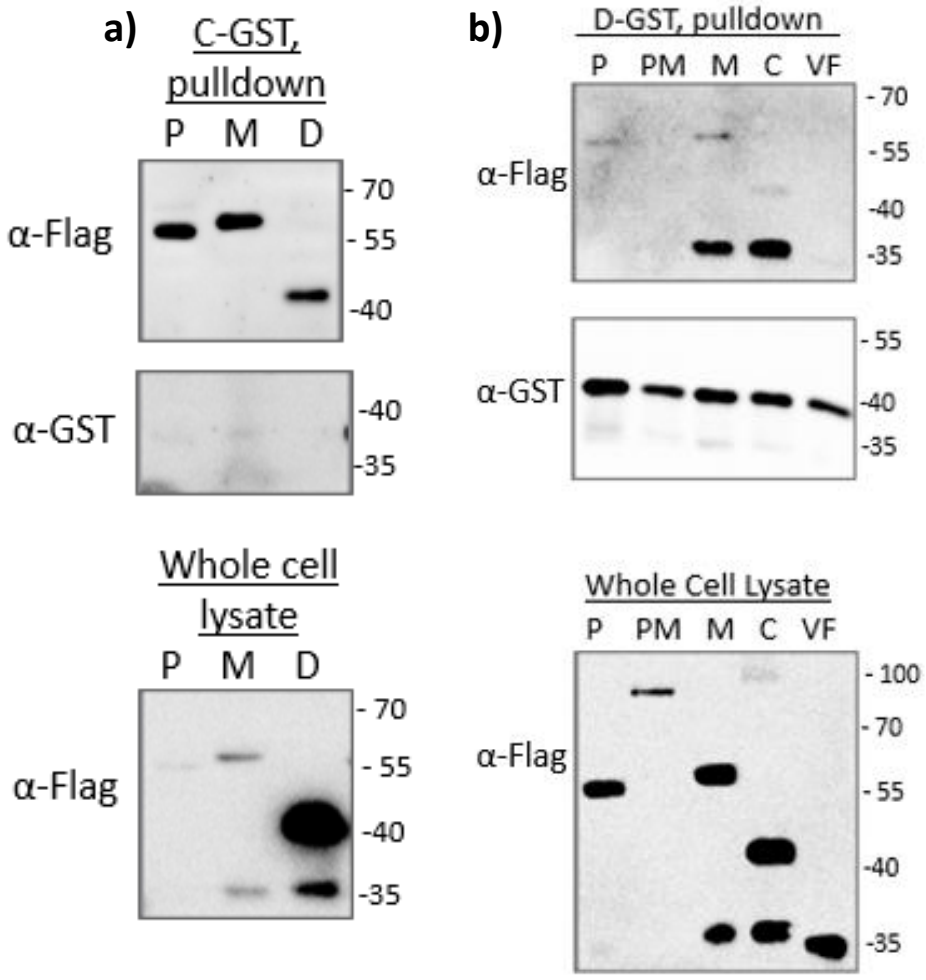

Supplementary Figure 3. GST Pulldown of other ADAM10 domain constructs paired. Protein domains that underwent pulldown are shown above and protein expression is shown below for each set a-b. a) Interaction of C-terminal GST-tagged C domain construct (C-GST) with respectively N-terminal VF tagged P, M, and D constructs. b) Interaction of C-terminal GST-tagged D domain construct (D-GST) with respectively N-terminal VF tagged P, PM, M, and C constructs. VF in each lane represent a control for each experimental set up.

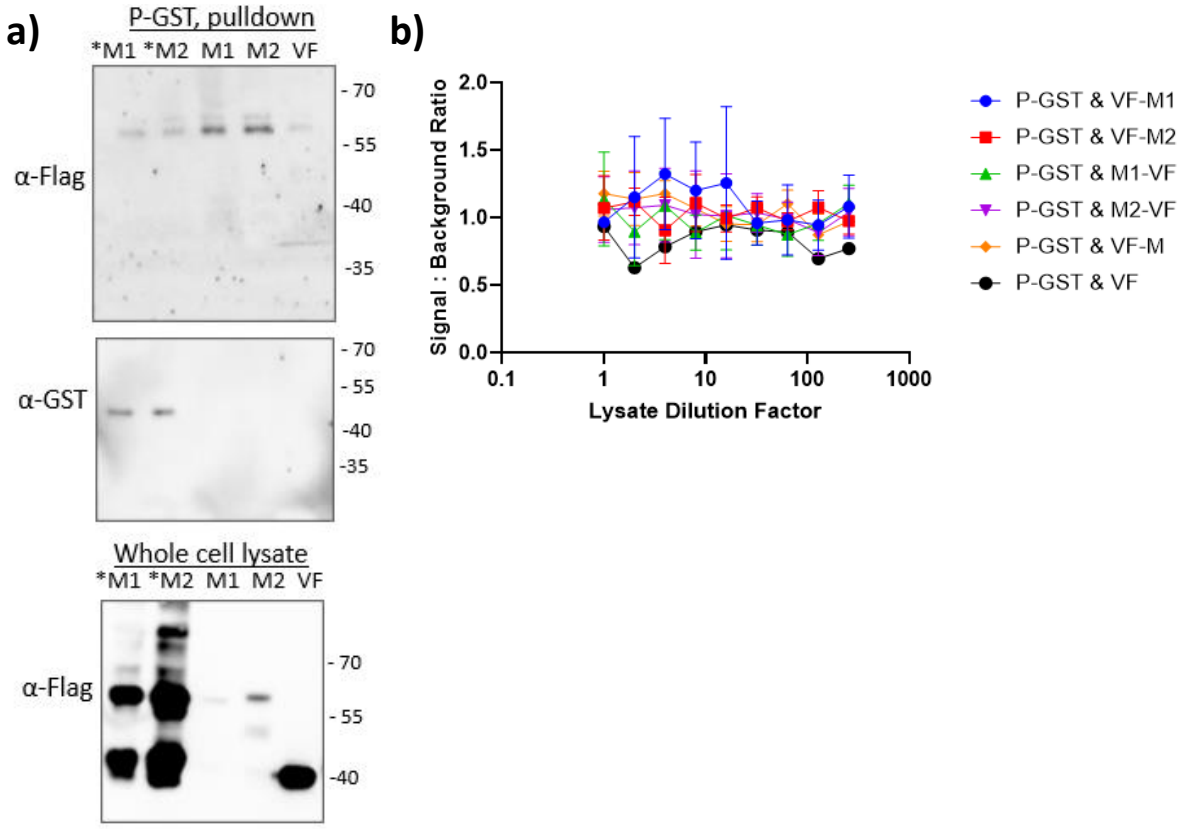

Supplementary Figure 4. P domain interacting with truncations of the M domain (M1 220-336) and M2 (337-459). a) Interaction of C-terminal GST-tagged P domain construct with respectively N-terminal VF tagged M1 and M2 labeled with an * (VF-M1 and VF-M2) and C-terminal VF tagged M1 and M2 constructs are labeled with no * (M1-VF and M2-VF). VF in each lane represents a control for each experimental set up. b) TR-FRET signals displayed of the interactions between C-terminal GST tagged P domains (P-GST) and VF-tagged constructs of M1 and M2 that are either N-terminal (VF-M1 and VF-M2) or C-terminal (M1-VF and M2-VF). All interactions tested consisted of 3 trials and the signals displayed represent the mean and standard deviation.

References:

1. Reprinted from “Gateway Cloning”, by BioRender.com (2022). Retrieved from https://app.biorender.com/biorender-templates. 2022.

2. Seegar, T. C. M.; Killingsworth, L. B.; Saha, N.; Meyer, P. A.; Patra, D.; Zimmerman, B.; Janes, P. W.; Rubinstein, E.; Nikolov, D. B.; Skiniotis, G.; Kruse, A. C.; Blacklow, S. C., Structural Basis for Regulated Proteolysis by the α-Secretase ADAM10. *Cell* **2017,** *171* (7), 1638-1648.e7.

3. Khachaturian, Z. S., Diagnosis of Alzheimer's disease. *Archives of neurology* **1985,** *42* (11), 1097-1105.

4. Nussbaum, R. L.; Ellis, C. E., Alzheimer's Disease and Parkinson's Disease. *New England Journal of Medicine* **2003,** *348* (14), 1356-1364.

5. Esteve, P.; Rueda-Carrasco, J.; Inés Mateo, M.; Martin-Bermejo, M. J.; Draffin, J.; Pereyra, G.; Sandonís, Á.; Crespo, I.; Moreno, I.; Aso, E.; Garcia-Esparcia, P.; Gomez-Tortosa, E.; Rábano, A.; Fortea, J.; Alcolea, D.; Lleo, A.; Heneka, M. T.; Valpuesta, J. M.; Esteban, J. A.; Ferrer, I.; Domínguez, M.; Bovolenta, P., Elevated levels of Secreted-Frizzled-Related-Protein 1 contribute to Alzheimer’s disease pathogenesis. *Nature Neuroscience* **2019,** *22* (8), 1258-1268.

6. Anand, R.; Gill, K. D.; Mahdi, A. A., Therapeutics of Alzheimer's disease: Past, present and future. *Neuropharmacology* **2014,** *76 Pt A*, 27-50.

7. Goedert, M.; Spillantini, M. G., A century of Alzheimer's disease. *science* **2006,** *314* (5800), 777-781.

8. Wenk, G. L., Neuropathologic changes in Alzheimer's disease. *Journal of Clinical Psychiatry* **2003,** *64*, 7-10.

9. Barenholtz Levy, H., Accelerated Approval of Aducanumab: Where Do We Stand Now? *Annals of Pharmacotherapy 0* (0), 10600280211050405.

10. Reiss, K.; Saftig, P., The "A Disintegrin And Metalloprotease" (ADAM) family of sheddases: Physiological and cellular functions. *Seminars in Cell & Developmental Biology* **2009,** *20* (2), 126-137.

11. Klein, T.; Bischoff, R., Active Metalloproteases of the A Disintegrin And Metalloprotease (ADAM) Family: Biological Function and Structure. *Journal of Proteome Research* **2011,** *10* (1), 17-33.

12. Wetzel, S.; Seipold, L.; Saftig, P., The metalloproteinase ADAM10: A useful therapeutic target? *Biochimica et Biophysica Acta (BBA) - Molecular Cell Research* **2017,** *1864* (11, Part B), 2071-2081.

13. Jorissen, E.; Prox, J.; Bernreuther, C.; Weber, S.; Schwanbeck, R.; Serneels, L.; Snellinx, A.; Craessaerts, K.; Thathiah, A.; Tesseur, I.; Bartsch, U.; Weskamp, G.; Blobel, C. P.; Glatzel, M.; De Strooper, B.; Saftig, P., The Disintegrin/Metalloproteinase ADAM10 Is Essential for the Establishment of the Brain Cortex. *The Journal of Neuroscience* **2010,** *30* (14), 4833-4844.

14. Saftig, P.; Lichtenthaler, S. F., The alpha secretase ADAM10: A metalloprotease with multiple functions in the brain. *Progress in Neurobiology* **2015,** *135*, 1-20.

15. Sogorb-Esteve, A.; García-Ayllón, M.-S.; Gobom, J.; Alom, J.; Zetterberg, H.; Blennow, K.; Sáez-Valero, J., Levels of ADAM10 are reduced in Alzheimer's disease CSF. *Journal of Neuroinflammation* **2018,** *15* (1), 213.

16. Tyler, S. J.; Dawbarn, D.; Wilcock, G. K.; Allen, S. J., α- and β-secretase: profound changes in Alzheimer's disease. *Biochemical and Biophysical Research Communications* **2002,** *299* (3), 373-376.

17. Tyler, S. J.; Dawbarn, D.; Wilcock, G. K.; Allen, S. J., alpha- and beta-secretase: profound changes in Alzheimer's disease. *Biochem Biophys Res Commun* **2002,** *299* (3), 373-6.

18. Colciaghi, F.; Borroni, B.; Pastorino, L.; Marcello, E.; Zimmermann, M.; Cattabeni, F.; Padovani, A.; Di Luca, M., α-Secretase ADAM10 as Well as αAPPs Is Reduced in Platelets and CSF of Alzheimer Disease Patients. *Molecular Medicine* **2002,** *8* (2), 67-74.

19. Asai, M.; Hattori, C.; Szabó, B.; Sasagawa, N.; Maruyama, K.; Tanuma, S.-i.; Ishiura, S., Putative function of ADAM9, ADAM10, and ADAM17 as APP α-secretase. *Biochemical and Biophysical Research Communications* **2003,** *301* (1), 231-235.

20. Yuan, X.-Z.; Sun, S.; Tan, C.-C.; Yu, J.-T.; Tan, L., The Role of ADAM10 in Alzheimer's Disease. *Journal of Alzheimer's Disease* **2017,** *58*, 303-322.

21. Kuhn, P.-H.; Wang, H.; Dislich, B.; Colombo, A.; Zeitschel, U.; Ellwart, J. W.; Kremmer, E.; Roßner, S.; Lichtenthaler, S. F., ADAM10 is the physiologically relevant, constitutive α-secretase of the amyloid precursor protein in primary neurons. *The EMBO Journal* **2010,** *29* (17), 3020-3032.

22. Hampel, H.; Hardy, J.; Blennow, K.; Chen, C.; Perry, G.; Kim, S. H.; Villemagne, V. L.; Aisen, P.; Vendruscolo, M.; Iwatsubo, T.; Masters, C. L.; Cho, M.; Lannfelt, L.; Cummings, J. L.; Vergallo, A., The Amyloid-β Pathway in Alzheimer's Disease. *Molecular Psychiatry* **2021,** *26* (10), 5481-5503.

23. Lichtenthaler, S. F., Alpha-secretase in Alzheimer's disease: molecular identity, regulation and therapeutic potential. *Journal of Neurochemistry* **2011,** *116* (1), 10-21.

24. Endres, K.; Deller, T., Regulation of Alpha-Secretase ADAM10 In vitro and In vivo: Genetic, Epigenetic, and Protein-Based Mechanisms. *Frontiers in Molecular Neuroscience* **2017,** *10*.

25. Postina, R.; Schroeder, A.; Dewachter, I.; Bohl, J.; Schmitt, U.; Kojro, E.; Prinzen, C.; Endres, K.; Hiemke, C.; Blessing, M.; Flamez, P.; Dequenne, A.; Godaux, E.; van Leuven, F.; Fahrenholz, F., A disintegrin-metalloproteinase prevents amyloid plaque formation and hippocampal defects in an Alzheimer disease mouse model. *The Journal of Clinical Investigation* **2004,** *113* (10), 1456-1464.

26. Tang, B. L., Enhancing α-secretase Processing for Alzheimer's Disease-A View on SFRP1. *Brain Sci* **2020,** *10* (2).

27. Vincent, B., Regulation of the α-secretase ADAM10 at transcriptional, translational and post-translational levels. *Brain Research Bulletin* **2016,** *126*, 154-169.

28. Marcade, M.; Bourdin, J.; Loiseau, N.; Peillon, H.; Rayer, A.; Drouin, D.; Schweighoffer, F.; Désiré, L., Etazolate, a neuroprotective drug linking GABAA receptor pharmacology to amyloid precursor protein processing. *Journal of Neurochemistry* **2008,** *106* (1), 392-404.

29. Hung, A. Y.; Haass, C.; Nitsch, R. M.; Qiu, W. Q.; Citron, M.; Wurtman, R. J.; Growdon, J. H.; Selkoe, D. J., Activation of protein kinase C inhibits cellular production of the amyloid beta-protein. *Journal of Biological Chemistry* **1993,** *268* (31), 22959-22962.

30. Etcheberrigaray, R.; Tan, M.; Dewachter, I.; Kuipéri, C.; Van der Auwera, I.; Wera, S.; Qiao, L.; Bank, B.; Nelson, T. J.; Kozikowski, A. P.; Van Leuven, F.; Alkon, D. L., Therapeutic effects of PKC activators in Alzheimer's disease transgenic mice. *Proc Natl Acad Sci U S A* **2004,** *101* (30), 11141-6.

31. Gallardo, G., Secreted frizzled-related protein 1 frazzles the brain in Alzheimer’s disease. *Science Translational Medicine* **2019,** *11* (504), eaay7697.

32. Marcos, S.; Nieto-Lopez, F.; Sandonìs, A.; Cardozo, M. J.; Di Marco, F.; Esteve, P.; Bovolenta, P., Secreted Frizzled Related Proteins Modulate Pathfinding and Fasciculation of Mouse Retina Ganglion Cell Axons by Direct and Indirect Mechanisms. *The Journal of Neuroscience* **2015,** *35* (11), 4729-4740.

33. Esteve, P.; Sandonìs, A.; Cardozo, M.; Malapeira, J.; Ibañez, C.; Crespo, I.; Marcos, S.; Gonzalez-Garcia, S.; Toribio, M. L.; Arribas, J.; Shimono, A.; Guerrero, I.; Bovolenta, P., SFRPs act as negative modulators of ADAM10 to regulate retinal neurogenesis. *Nature Neuroscience* **2011,** *14* (5), 562-569.

34. Jia, L.; Piña-Crespo, J.; Li, Y., Restoring Wnt/β-catenin signaling is a promising therapeutic strategy for Alzheimer's disease. *Mol Brain* **2019,** *12* (1), 104.

35. Seals, D. F.; Courtneidge, S. A., The ADAMs family of metalloproteases: multidomain proteins with multiple functions. *Genes Dev* **2003,** *17* (1), 7-30.

36. Stawikowska, R.; Cudic, M.; Giulianotti, M.; Houghten, R. A.; Fields, G. B.; Minond, D., Activity of ADAM17 (a Disintegrin and Metalloprotease 17) Is Regulated by Its Noncatalytic Domains and Secondary Structure of its Substrates*. *Journal of Biological Chemistry* **2013,** *288* (31), 22871-22879.

37. Moss, M. L.; Bomar, M.; Liu, Q.; Sage, H.; Dempsey, P.; Lenhart, P. M.; Gillispie, P. A.; Stoeck, A.; Wildeboer, D.; Bartsch, J. W.; Palmisano, R.; Zhou, P., The ADAM10 Prodomain Is a Specific Inhibitor of ADAM10 Proteolytic Activity and Inhibits Cellular Shedding Events *. *Journal of Biological Chemistry* **2007,** *282* (49), 35712-35721.

38. Anders, A.; Gilbert, S.; Garten, W.; Postina, R.; Fahrenholz, F., Regulation of the α-secretase ADAM10 by its prodomain and proprotein convertases. *The FASEB Journal* **2001,** *15* (10), 1837-1839.

39. FAHRENHOLZ, F.; GILBERT, S.; KOJRO, E.; LAMMICH, S.; POSTINA, R., α-Secretase Activity of the Disintegrin Metalloprotease ADAM 10: Influences of Domain Structure. *Annals of the New York Academy of Sciences* **2000,** *920* (1), 215-222.

40. Smith , K. M.; Gaultier , A.; Cousin , H.; Alfandari , D.; White , J. M.; DeSimone , D. W., The cysteine-rich domain regulates ADAM protease function in vivo. *Journal of Cell Biology* **2002,** *159* (5), 893-902.

41. Adapted from "AAV Production by Triple Transfection", by BioRender.com (2022). Retrieved from https://app.biorender.com/biorender-templates. 2022.

42. Adapted from "Glutathione-S-transferase (GST) pull-down assay", by BioRender.com (2022). Retrieved from https://app.biorender.com/biorender-templates. 2022.

43. Adapted from "TR-FRET Assay", by BioRender.com (2022). Retrieved from https://app.biorender.com/biorender-templates. 2022.

44. Hooper, N. M.; Turner, A. J., The Search for α-Secretase and its Potential as a Therapeutic Approach to Alzheimer's Disease. *Current Medicinal Chemistry* **2002,** *9* (11), 1107-1119.

45. Allinson, T. M.; Parkin, E. T.; Turner, A. J.; Hooper, N. M., ADAMs family members as amyloid precursor protein alpha-secretases. *J Neurosci Res* **2003,** *74* (3), 342-52.

46. Peron, R.; Vatanabe, I. P.; Manzine, P. R.; Camins, A.; Cominetti, M. R., Alpha-Secretase ADAM10 Regulation: Insights into Alzheimer's Disease Treatment. *Pharmaceuticals* **2018,** *11* (1), 12.

47. Endres, K.; Fahrenholz, F., Upregulation of the α-secretase ADAM10 – risk or reason for hope? *The FEBS Journal* **2010,** *277* (7), 1585-1596.

48. Seegar, T. C.; Blacklow, S. C., Domain integration of ADAM family proteins: Emerging themes from structural studies. *Exp Biol Med (Maywood)* **2019,** *244* (17), 1510-1519.

49. Janes, P. W.; Saha, N.; Barton, W. A.; Kolev, M. V.; Wimmer-Kleikamp, S. H.; Nievergall, E.; Blobel, C. P.; Himanen, J.-P.; Lackmann, M.; Nikolov, D. B., Adam Meets Eph: An ADAM Substrate Recognition Module Acts as a Molecular Switch for Ephrin Cleavage In trans. *Cell* **2005,** *123* (2), 291-304.

50. Tape, C. J.; Willems, S. H.; Dombernowsky, S. L.; Stanley, P. L.; Fogarasi, M.; Ouwehand, W.; McCafferty, J.; Murphy, G., Cross-domain inhibition of TACE ectodomain. *Proceedings of the National Academy of Sciences* **2011,** *108* (14), 5578-5583.

51. Pan, D.; Rubin, G. M., Kuzbanian controls proteolytic processing of Notch and mediates lateral inhibition during Drosophila and vertebrate neurogenesis. *Cell* **1997,** *90* (2), 271-80.